Preprint typeset in JINST style - HYPER VERSION

CALICE Analysis Note CAN-038
October 18, 2012

The Time Structure of Hadronic Showers in Tungsten and Steel with T3B

The CALICE Collaboration*

This note contains preliminary CALICE results, and is for the use of members of the CALICE Collaboration and others to whom permission has been given.

ABSTRACT: We present results on the time structure of hadronic showers in tungsten and steel measured with the T3B setup installed behind the CALICE WAHCAL and the CALICE SDHCAL. These results are compared to Geant4 simulations using different physics lists.

*Corresponding authors: Frank Simon (fsimon@mpp.mpg.de), Christian Soldner (soldner@mpp.mpg.de), Lars Weuste (weuste@mpp.mpg.de)

Contents

1. Introduction

The intrinsic time structure of hadronic showers can provide fundamental limitations on the time resolution achievable with hadronic calorimeters, which are relevant for future colliders with challenging collision bunch structure and high background rates such as CLIC [1]. Since the performance of detectors at such facilities are evaluated using Geant4 simulations, a validation of the quality of the reproduction of the time structure by the physics models is highly relevant. The T3B experiment has already provided first results of the time structure in a scintillator-tungsten sampling calorimeter for low hadron energies [2]. These results are here improved with higher statistics at higher energies recorded at the CERN SPS, and are extended by comparisons of tungsten and steel absorbers. In addition, by a matching of events recorded in T3B and in the CALICE scintillator tungsten calorimeter the shower starting point can be determined, providing measurements as a function of shower depth relative to the first inelastic interaction.

The data presented here were recorded in Summer and Fall 2011 with the CALICE scintillator tungsten calorimeter (WHCAL) prototype [3, 4] and with the CALICE RPC steel semi-digital calorimeter (SDHCAL) prototype [5]. Due to different DAQ systems and due to, at that time, limited data taking rate of the SDHCAL, an event-wise correlation of the data is only possible with the WHCAL.

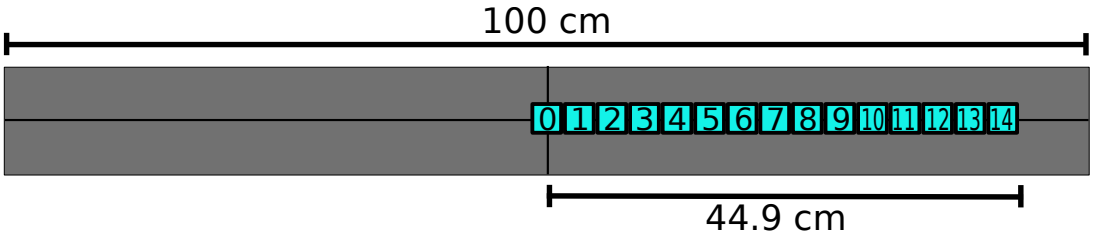

Figure 1. Layout of the T3B scintillator tiles. From the nominal beam axis, the setup extends by 15 mm to one and 449 mm to the other side.

2. Experimental Setup

The T3B setup consists of fifteen 3×3 cm^2 scintillator tiles with a thickness of 5 mm, directly read out with 1 mm^2 Hamamatsu MPPC50P SiPMs with four hundred 50×50 μm^2 pixels to achieve higher sensitivity for low energy deposits compared to the more conventional use of SiPMs with 1000 or more pixels. The scintillator tiles are arranged in one row extending from the center of the calorimeter horizontally out to one side of the detector with 1 mm space between tiles, providing full coverage of the radial extent of showers out to a radius of 449 mm, as illustrated in Figure 1. The full setup is read out with four 4-channel USB oscilloscopes[1] with 800 ps sampling, recording 2.4 μs per event to provide information also on very late components of the hadronic shower. The setup is described in more detail in [2].

T3B is installed behind the main calorimeter. In the case of the WHCAL, this is after 38 absorber layers, amounting to a depth of approximately 5 λ_I, 1 m from the front face of the calorimeter. Behind T3B, at a distance of 9 cm, follows a scintillator-steel tail catcher. In the case of the SDHCAL, T3B sits after 50 absorber layers, 40 out of which are equipped with GRPC modules for readout, with a depth of approximately 6 λ_I, 1.4 m from the front face of the detector.

3. Data Analysis

The data analysis is performed by decomposing the recorded waveforms of each channel into individual single-photon events with a time-stamp with a 800 ps precision, as described in detail in [2]. In the decomposition an automatic gain correction is applied by using reference single-photon signals recorded between spills during the data taking. The additional temperature dependence of the signal not taken into account by the gain correction is corrected for using temperature coefficients from laboratory measurements. At this stage, energy deposits are transformed to the MIP scale, determined in laboratory measurements with a ^{90}Sr source and from muon reference runs.

As previously, the study is based on the time of first hit, meaning that only the first hit in a tile per event is considered. This makes the analysis very robust against the influence of afterpulses from the photon sensors and other detector effects that may lead to late signals, correlated to an earlier signal. The time of this hit is taken from the timing of the second identified photon. With this requirement, the sensitivity to single-p.e. noise events close to the identified hit is reduced. A valid hit is required to have an amplitude of at least 8 photons, corresponding to around 0.4 MIP,

[1] PicoTech PicoScope 6403 (http://www.picotech.com/)

over 9.6 ns. Using only the first hit does not lead to a substantial loss of information. A study investigating multiple hits has shown that only about 3% of all first hits are followed by a second hit with an amplitude of at least 30% of that of the original hit within the recording time of the data acquisition. The presence of afterpulses makes the reconstruction of these hits less precise at present, which is why they are not considered in the analysis.

Since the absolute time difference between the passage of the particle and the T3B readout is not known, the timing relative to the trigger is determined from data. $t = 0$ is defined by the position of the maximum of the prompt energy deposition peak, determined by a simple peak finder. Since different trigger configurations were used for different data samples, this is performed for each data sample (muons, steel, tungsten) separately. The systematic uncertainties of this $t = 0$ determination are estimated to be at the level of 100 ps to 200 ps.

Here, a data set of 4.06 million 60 GeV π^+ events is analyzed in the case of the WAHCAL and 1.6 million 60 GeV π^+ events in the case of the SDHCAL. In addition, 5.4 million muon events recorded with T3B behind the SDHCAL are used as reference data. No particle identification is performed, meaning that the hadronic data sample includes an admixture of protons, muons, positrons and kaons for all analyses described here.

Simulations are performed using Geant4.9.4p03 with three physics lists: QBBC, QGSP_BERT, QGSP_BERT_HP, with 2 million pion events each. The simulation procedure has been refined compared to [2], using an improved model of the cell response to instantaneous energy deposits derived with a more realistic function from muon data. This function, consisting of an error function multiplied with three exponential functions with different offsets and different slopes, provides a good fit to the time evolution of the response to muons over the full time window of the data acquisition. Since the muon trigger used in the experiment has a larger time jitter than the hadron trigger, and since there are some subtle differences between data and simulations introduced by the limited vertical range of the picoscopes, the mean time of first hit in simulations (introduced in detail below) is slightly biased compared to data. This is corrected by an offset of 290 ps applied to all mean hit times in simulations. In addition to the digitization, also the geometry description has been improved with a realistic model of the T3B layer and of the other calorimeters. In the case of the WAHCAL, the tail catcher behind T3B is also modeled. In the simulation of the scintillator response the attenuation of signals of slow particles following Birk's law is included.

Data and simulations are corrected for a hit-amplitude dependent time-slewing effect. The correction function for this is determined from the amplitude-dependent mean time of the first observed hit in muon data and simulations.

4. Results

Figure 2 shows the distribution of the reconstructed time of first hit as a function of the energy of the hit for pions in steel and tungsten as well as the reference distribution for muons. Here, all T3B cells are combined into the plot. To allow a direct comparison of the distributions, all three histograms have the same number of entries. Separated by tile number, these distributions form the basis of all following analysis, which studies different projections of these distributions. From Figure 2 it is already apparent that hadronic showers exhibit substantial late contributions, in

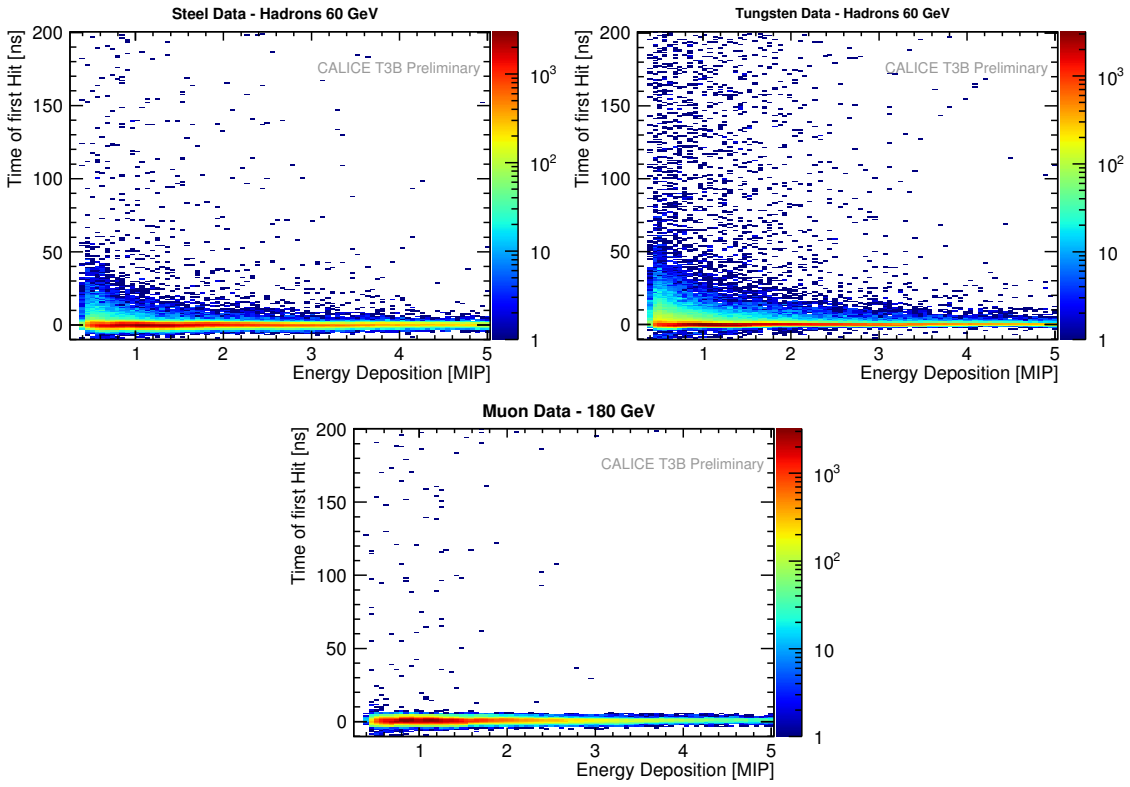

Figure 2. Identified first hits in T3B as a function of hit amplitude and hit time. Upper row: Distributions for 60 GeV π^+ with steel absorber (*left*) and tungsten absorber (*right*). Lower row: Reference distribution for 180 GeV muons with steel absorber. All three plots have the same number of entries (203 103 events with at least one T3B hit).

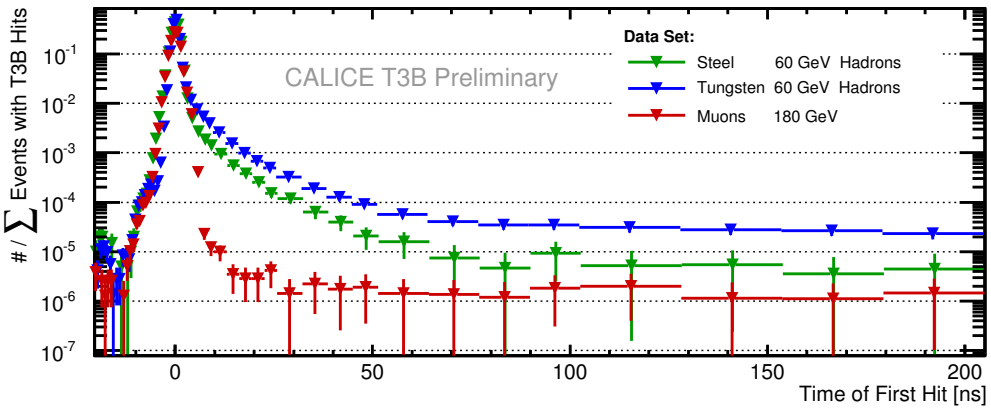

Figure 3. Distribution of the time of first hit in T3B for 60 GeV π^+ in steel and tungsten, compared to reference data from 180 GeV muons in steel. All distributions are normalized to the number of events which have at least one hit in T3B, which provides a comparison of the shape rather than the overall hit probability.

particular at low energy. The time structure in tungsten is considerably richer than that observed in steel.

This is also clearly seen in Figure 3, which shows the distribution of the time of first hit in the T3B module for hadrons in steel and tungsten as well as for muons. The response to muons is very fast, with most of the energy reconstructed within a few nanoseconds, giving an impression of the intrinsic time resolution of the combined system including triggers, scintillator and photon sensor response and photon reconstruction. Compared to this, the response to hadrons shows a long tail to later times, which is substantially more pronounced in the case of tungsten absorbers. Approximately 15 ns after the trigger, the number of late hits in tungsten exceeds that in steel by a factor of three, increasing even further for later times.

The energy dependence of the timing of hits is studied in Figure 4, by showing the distribution of the time of first hit as shown in Figure 3 for three different energy ranges. As expected there is no energy dependence for muons, since all signals are instantaneous, irrespective of the amount of energy deposited by the minimum-ionizing particles. For hadrons, the shape of the distribution depends strongly on energy. In both absorbers, late hits are predominantly of low energy. While in steel only energy deposits up to 2 MIP (1.6 MeV) show a considerable late component, in tungsten also higher-energy hits have substantial late contributions.

The mean time of first hit has proven to be a good observable to study the time structure in data and simulations with additional degrees of freedom, such as radial distance from the shower core or the energy of hits. The energy dependence of the time structure is shown in a compact way in Figure 5 by the mean time of first hit for pions in the WAHCAL and the SDHCAL as well as the muon reference. The mean time of first hit for steel quickly approaches that for muons, with only small effects from late energy deposits visible above 1 MIP. For tungsten, substantial contributions of late hits are also present at higher energies.

Figure 6 illustrates the lateral dependence of the time structure of hadronic showers in steel and tungsten by showing the mean time of first hit as a function of distance from the beam axis. In both absorbers, late energy deposits are more important in the outer region of the shower. In tungsten, the increase in the mean time of first hit with radius is substantially more pronounced than in steel.

5. Comparison to Simulations

The comparison to simulations provides crucial information on the level of realism of the considered Geant4 physics models concerning the time evolution of showers. This is particularly important for the study of detector concepts where timing is critical.

Figure 7 shows the distribution of the time of first hit in all T3B cells combined for 60 GeV positive hadrons in steel and tungsten. The distributions are compared to Geant4 simulations using the three different physics lists considered in the present note. For steel absorbers, satisfactory agreement is observed for all physics lists, with excellent agreement provided by QGSP_BERT_HP and QBBC over the full time range considered. For tungsten, only QBBC and QGSP_BERT_HP are able to reproduce the observed behavior, while QGSP_BERT without high precision neutron treatment predicts too much late shower activity.

Figure 8 shows the mean time of first hit as a function of radial distance from the beam axis for hadronic showers in steel and tungsten compared to simulations. When comparing steel and tungsten in the figure, one has to keep the geometrical differences between the two calorimeter setups

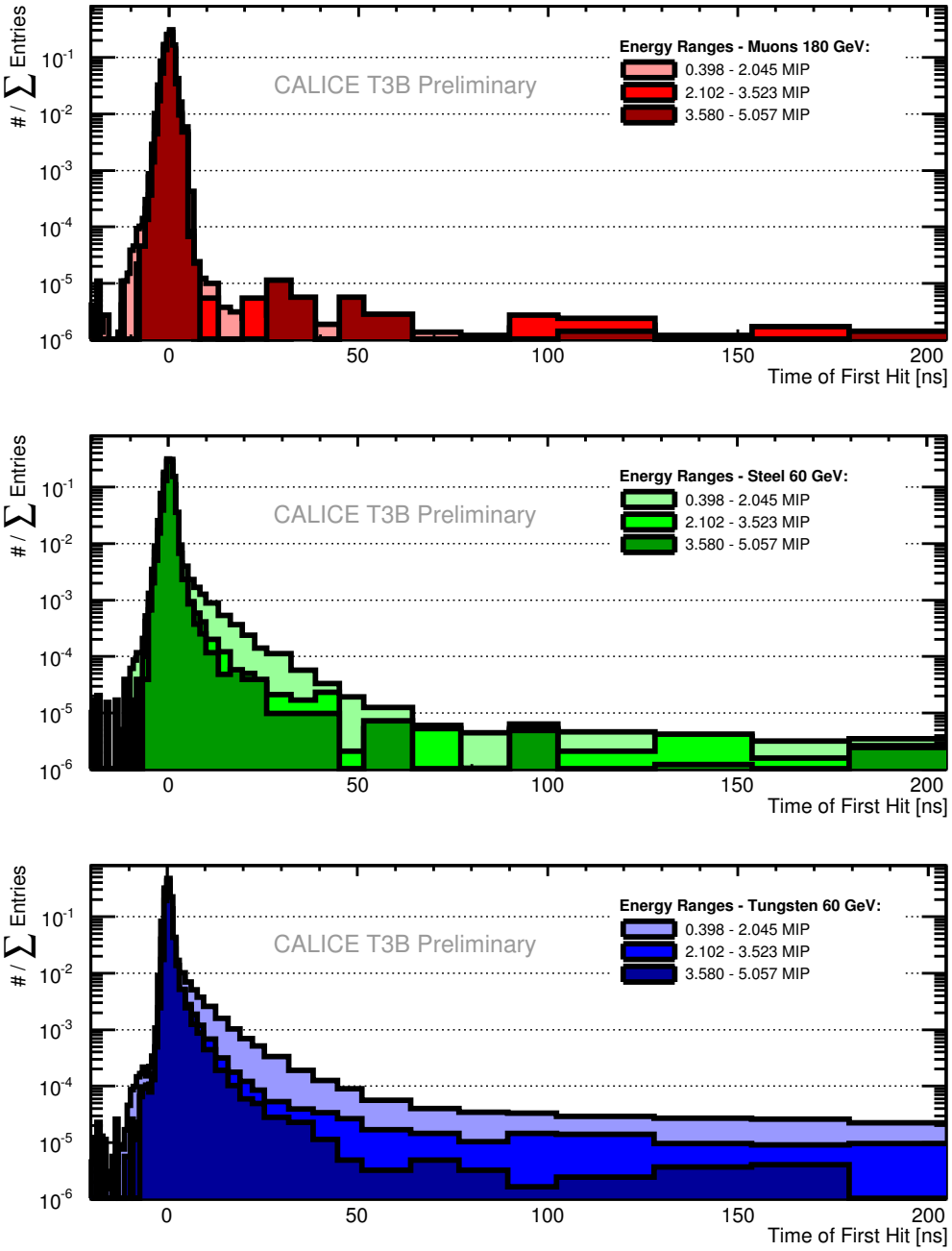

Figure 4. Distribution of the time of first hit in T3B for three different hit energy ranges, corresponding to energy deposits up to 1.6 MeV, from 1.6 MeV to 2.9 MeV and from 2.9 MeV to 4.1 MeV in the scintillator cell. From top to bottom 180 GeV muons in steel, 60 GeV π^+ in steel and in tungsten.

in mind, where the steel calorimeter is 40% longer than the tungsten one. For simple geometrical time-of-propagation effects, this would mean that the values at a radius of 300 mm in tungsten should be compared to those above 400 mm in steel. However, the time structure is largely due to other effects, as seen in both simulations and data by the absence of a strong dependence of the

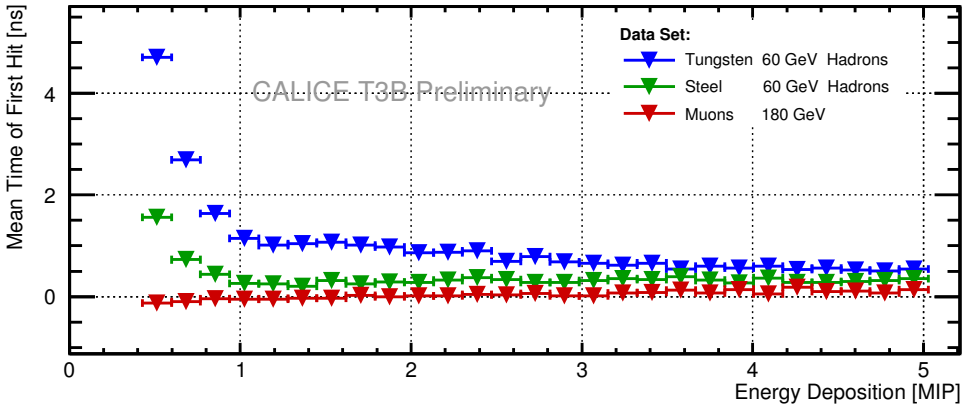

Figure 5. Mean time of first hit in T3B as a function of hit energy for pions in steel and tungsten as well as muons for reference.

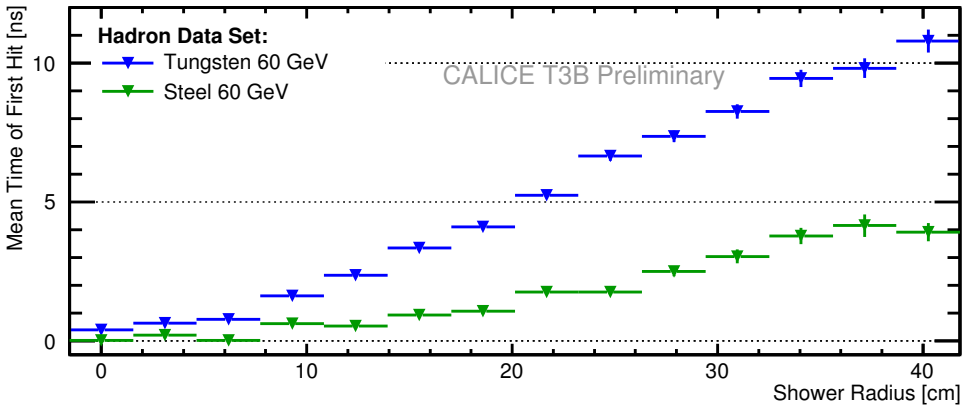

Figure 6. Mean time of first hit as a function of the radial distance from the beam axis for showers in steel and tungsten.

mean time of first hit in the outer regions of the shower from the shower depth. In general, the mean time of first hit increases with increasing radius. This is expected since prompt electromagnetic shower components and highly energetic secondary hadrons contribute mostly close to the beam axis, while neutrons and other low-energetic particles responsible for late shower components spread further from the shower core. The increase with increasing radius is more pronounced in tungsten than in steel, in line with the observation of greater late shower activity in tungsten discussed above. While all physics models reproduce the behavior in steel very well, the QGSP_BERT physics list fails to reproduce the distribution in tungsten, overestimating late shower activity in the outer regions of the shower.

The energy dependence of the mean time of first hit compared to simulations is shown in Figure 9. As for the other distributions, the steel data is well reproduced by all physics lists, while QGSP_BERT fails to reproduce the tungsten data.

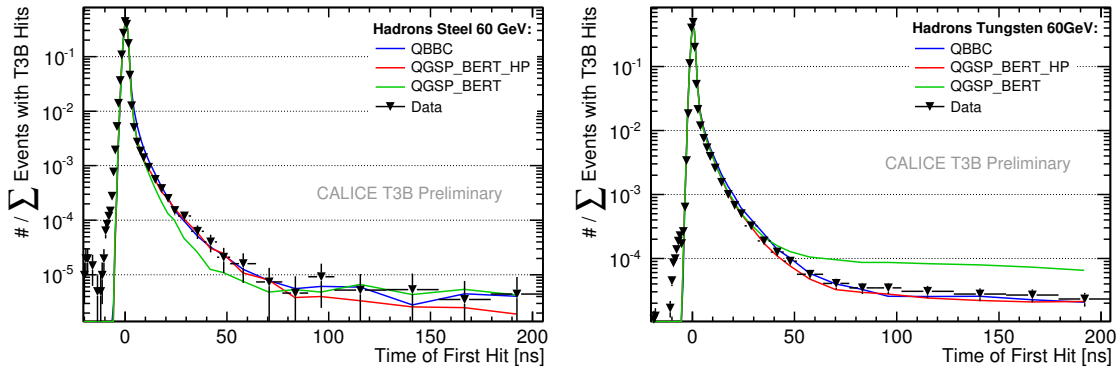

Figure 7. Distribution of the time of first hit in T3B for 60 GeV π^+ in steel and tungsten, compared to Geant4 simulations with different physics lists. All distributions are normalized to the number of events which have at least one hit in T3B, which provides a comparison of the shape rather than the overall hit probability.

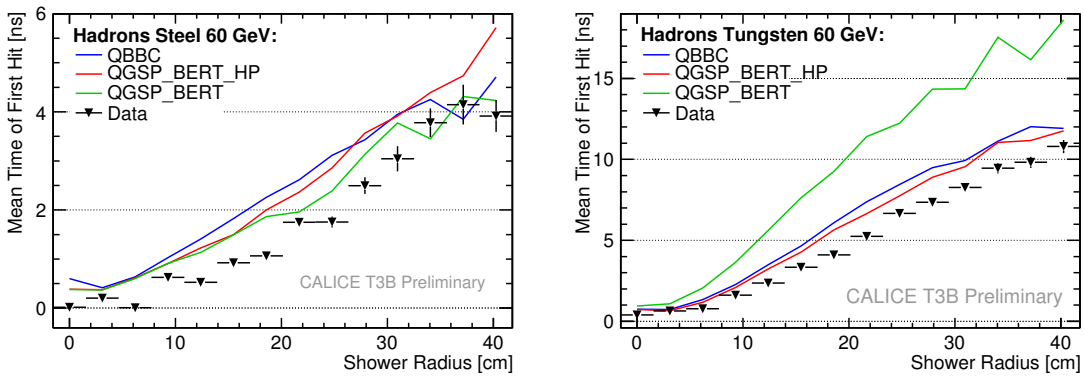

Figure 8. Mean time of first hit as a function of the radial distance from the beam axis in steel and tungsten, compared to Geant4 simulations with different physics lists. Geometrical differences of the different calorimeter setups for steel and tungsten absorbers are not corrected for, see text for more details.

6. Time Structure vs Depth from Shower Start in Tungsten

The possibility to match events recorded in T3B with events in the WAHCAL enables the time evolution to be studied as a function of shower depth relative to the first inelastic interaction, using the shower start determined in the WAHCAL. The event matching in the analysis is performed in two steps. Since the T3B readout system cannot provide event-wise time stamps, in the first step spills are matched based on time. Events within the spill are matched sequentially if the number of events recorded in T3B and in the WAHCAL is identical for that particular spill. Since T3B also records the trigger scintillator coincidence in addition to the main calorimeter trigger, calibration triggers that may occur during the spill are ignored in the matching. The shower start in the WAHCAL is determined using the standard CALICE shower start finder [6], which provides a resolution of ± 1 layer for the majority of events. For simulated data, the location of the shower start is taken to be the position of the first inelastic interaction taken directly from Geant4, smeared

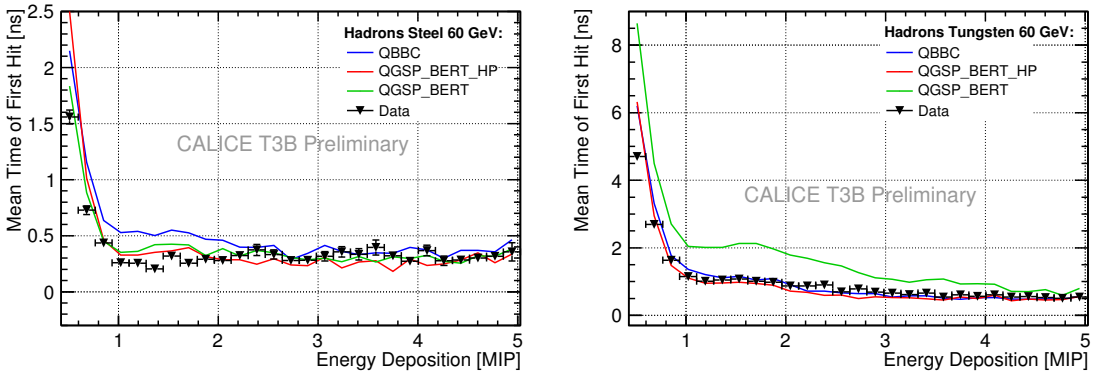

Figure 9. Mean time of first hit in all T3B cells as a function of the hit amplitude, compared to Geant4 simulations with different physics lists.

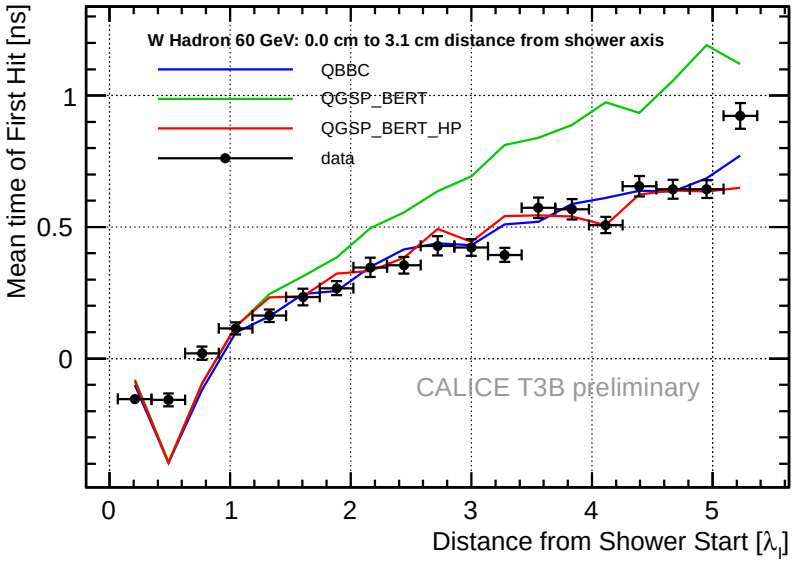

Figure 10. Mean time of first hit along the beam axis measured in the central tile of T3B as a function of depth in the hadronic shower, compared to Geant4 simulations with different physics lists.

with a gaussian with a sigma of 1 layer. The depth of the measurement in one particular event is determined by the distance between T3B and the identified shower start. By combining large data samples, the full (average) time structure of a hadronic shower up to the depth of T3B, i.e. 5 λ_I, can be determined.

Figure 10 shows the evolution of the time of first hit with depth along the beam axis (measured in tile 0 as shown in Figure 1), compared to simulations. The data shows a slow increase of the time of first hit going from the shower front to the rear. This is attributed to the increased relative importance of late shower components further away from the primary inelastic interaction. This general trend of the distribution is reproduced by all physics lists. However, as seen for other observables as well, QGSP_BERT without high precision neutron treatment provides too much

late shower activity, here resulting in a more pronounced rise of the mean time of first hit towards the rear of the shower. For showers starting very close to T3B, the simulations exhibit a clear dip in the mean time of first hit which is not seen in data. This is caused by differences in the signal amplitude dependent time slewing correction in data and simulations due to saturation effects in the data acquisition and resulting differences in the number of high-amplitude hits.

7. Summary

T3B has expanded its studies of the time structure of hadronic showers at higher energies at the SPS, providing results both with steel and with tungsten absorbers. The time structure in tungsten is observed to be significantly different from the one in steel, with considerable late contributions at low energies as well as extending into the several MeV region. In steel, late shower contributions are predominantly low-energetic, comparable to or below the energy lost by a minimum-ionizing particle in the T3B scintillators. In tungsten, measurements as a function of the depth in the hadronic shower are possible, showing that the importance of late shower contributions increase towards the rear of the shower. Comparison to simulations show that the time structure in steel is in general well reproduced by the Geant4 physics lists QGSP_BERT, QGSP_BERT_HP and QBBC. In tungsten, only QGSP_BERT_HP and QBBC are able to reproduce the data on a satisfactory level, demonstrating that here a more sophisticated treatment of neutrons is necessary,

Acknowledgements

The research leading to these results has received funding from the European Commission under the FP7 Research Infrastructures project AIDA, grant agreement no. 262025 and by the DFG Cluster of Excellence "Origin and Structure of the Universe".

References

[1] P. Lebrun, L. Linssen, A. Lucaci-Timoce, D. Schulte, F. Simon, *et. al.*, *The CLIC Programme: Towards a Staged e^+e^- Linear Collider Exploring the Terascale : CLIC Conceptual Design Report*, arXiv:1209.2543.

[2] CALICE Collaboration, *First T3B Results - Initial Study of the Time of First Hit in a Scintillator-Tungsten HCAL*, *CALICE Analysis Note CAN-033 (2011)*.

[3] CALICE Collaboration, C. Adloff *et. al.*, *Construction and Commissioning of the CALICE Analog Hadron Calorimeter Prototype*, *JINST* **5** (2010) P05004, [arXiv:1003.2662].

[4] CALICE Collaboration, *Shower development of particles with momenta from 1 to 10 GeV in the CALICE Scintillator-Tungsten HCAL*, *CALICE Analysis Note CAN-036 (2012)*.

[5] I. Laktineh, *Construction of a technological semi-digital hadronic calorimeter using GRPC*, *J. Phys. Conf. Ser.* **293** (2011) 012077.

[6] CALICE Collaboration, C. Adloff *et. al.*, *Tests of a particle flow algorithm with CALICE test beam data*, *JINST* **6** (2011) P07005, [arXiv:1105.3417].